

9.2. Layer stacking

By S. ĐUROVIČ, P. KRISHNA AND D. PANDEY

9.2.1. Layer stacking in close-packed structures (By D. Pandey and P. Krishna)

The crystal structures of a large number of materials can be described in terms of stacking of layers of atoms. This chapter provides a brief account of layer stacking in materials with structures based on the geometrical principle of close packing of equal spheres.

9.2.1.1. Close packing of equal spheres

9.2.1.1.1. Close-packed layer

In a close-packed layer of spheres, each sphere is in contact with six other spheres as shown in Fig. 9.2.1.1. This is the highest number of nearest neighbours for a layer of identical spheres and therefore yields the highest packing density. A single close-packed layer of spheres has two-, three- and sixfold axes of rotation normal to its plane. This is depicted in Fig. 9.2.1.2(a), where the size of the spheres is reduced for clarity. There are three symmetry planes with indices $(1\bar{2}.0)$, $(\bar{2}1.0)$, and (11.0) defined with respect to the smallest two-dimensional hexagonal unit cell shown in Fig. 9.2.1.2(b). The point-group symmetry of this layer is $6mm$ and it has a hexagonal lattice. As such, a layer with such an arrangement of spheres is often called a hexagonal close-packed layer. We shall designate the positions of spheres in the layer shown in Fig. 9.2.1.1 by the letter 'A'. This A layer has two types of triangular interstices, one with the apex angle up (Δ) and the other with the apex angle down (∇). All interstices of one kind are related by the same hexagonal lattice as that for the A layer. Let the positions of layers with centres of spheres above the centres of the Δ and ∇ interstices be designated as 'B' and 'C', respectively. In the cell of the A layer shown in Fig. 9.2.1.1 ($a = b = \text{diameter of the sphere}$ and $\gamma = 120^\circ$), the three positions A, B, and C on projection have coordinates $(0, 0)$, $(\frac{1}{3}, \frac{2}{3})$, and $(\frac{2}{3}, \frac{1}{3})$, respectively.

9.2.1.1.2. Close-packed structures

A three-dimensional close-packed structure results from stacking the hexagonal close-packed layers in the A, B, or C position with the restriction that no two successive layers are in identical positions. Thus, any sequence of the letters A, B, and C, with no two successive letters alike, represents a possible manner of stacking the hexagonal close-packed layers. There are thus infinite possibilities for close-packed layer stackings. The

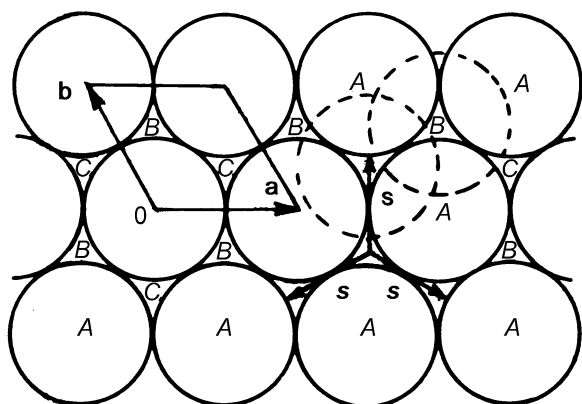


Fig. 9.2.1.1. The close packing of equal spheres in a plane.

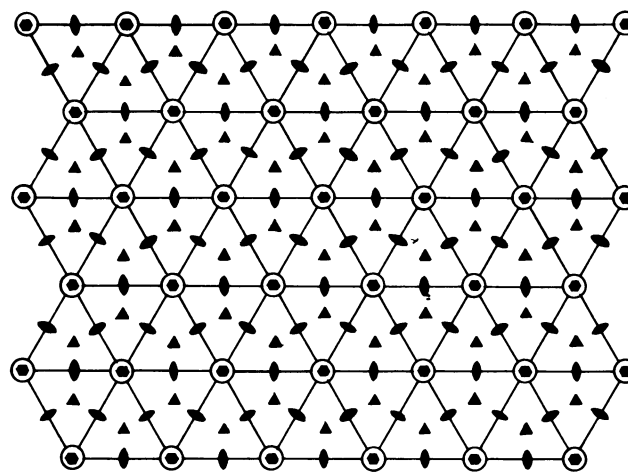
identity period n of these layer stackings is determined by the number of layers after which the stacking sequence starts repeating itself. Since there are two possible positions for a new layer on the top of the preceding layer, the total number of possible layer stackings with a repeat period of n is 2^{n-1} .

In all the close-packed layer stackings, each sphere is surrounded by 12 other spheres. However, it is touched by all 12 spheres only if the axial ratio h/a is $\sqrt{2/3}$, where h is the separation between two close-packed layers and a is the diameter of the spheres (Verma & Krishna, 1966). Deviations from the ideal value of the axial ratio are common, especially in hexagonal metals (Cottrell, 1967). The arrangement of spheres described above provides the highest packing density of 0.7405 in the ideal case for an infinite lattice (Azaroff, 1960). There are, however, other arrangements of a finite number of equal spheres that have a higher packing density (Boerdijk, 1952).

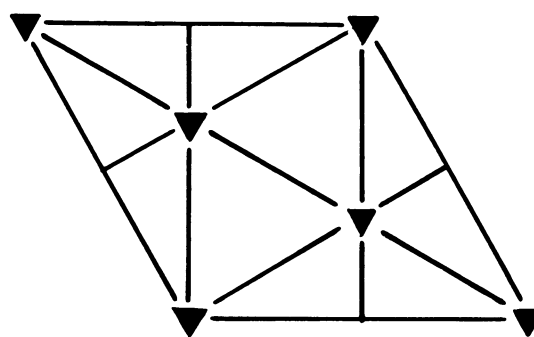
9.2.1.1.3. Notations for close-packed structures

In the Ramsdell notation, close-packed structures are designated as nX , where n is the identity period and X stands for the lattice type, which, as shown later, can be hexagonal (H), rhombohedral (R), or in one special case cubic (C) (Ramsdell, 1947).

In the Zhdanov notation, use is made of the stacking offset vector s and its opposite $-s$, which cause, respectively, a



(a)



(b)

Fig. 9.2.1.2. (a) Symmetry axes of a single close-packed layer of spheres and (b) the minimum axes symmetry of a three-dimensional close packing of spheres.

9.2. LAYER STACKING

Table 9.2.1.1. Common close-packed metallic structures

Stacking sequence	Identity period	Ramsdell notation	Zhdanov notation	Jagodzinski notation	Prototype
$AB, A \dots$	2	$2H$	11	h	Mg
$ABC, A \dots$	3	$3C$	∞	c	Cu
$ABCB, A \dots$	4	$4H$	22	hc	La
$ABCBCACAB, A \dots$	9	$9R$	21	hhc	Sm

cyclic ($A \rightarrow B \rightarrow C \rightarrow A$) or anticyclic ($A \rightarrow C \rightarrow B \rightarrow A$) shift of layers in the same plane. The vector s can be either $(1/3)[1\bar{1}00]$, $(1/3)[01\bar{1}0]$, or $(1/3)[\bar{1}010]$. Zhdanov (1945) suggested summing the number of consecutive offsets of each kind and designating them by numeral figures. Successive numbers in the Zhdanov symbol have opposite signs. The rhombohedral stackings have three identical sets of Zhdanov symbols in an identity period. It is usually sufficient to write only one set.

Yet another notation advanced, amongst others, by Jagodzinski (1949a) makes use of configurational symbols for each layer. A layer is designated by the symbol h or c according as its neighbouring layers are alike or different. Letter 'k' in place of 'c' is also used in the literature.

Some of the common close-packed structures observed in metals are listed in Table 9.2.1.1 in terms of all the notations.

9.2.1.2. Structure of compounds based on close-packed layer stackings

Frequently, the positions of one kind of atom or ion in inorganic compounds, such as SiC, ZnS, CdI₂, and GaSe, correspond approximately to those of equal spheres in a close packing, with the other atoms being distributed in the voids. All such structures will also be referred to as close-packed structures though they may not be ideally close packed. In the close-packed compounds, the size and coordination number of the smaller atom/ion may require that its close-packed neighbours in the neighbouring layers do not touch each other.

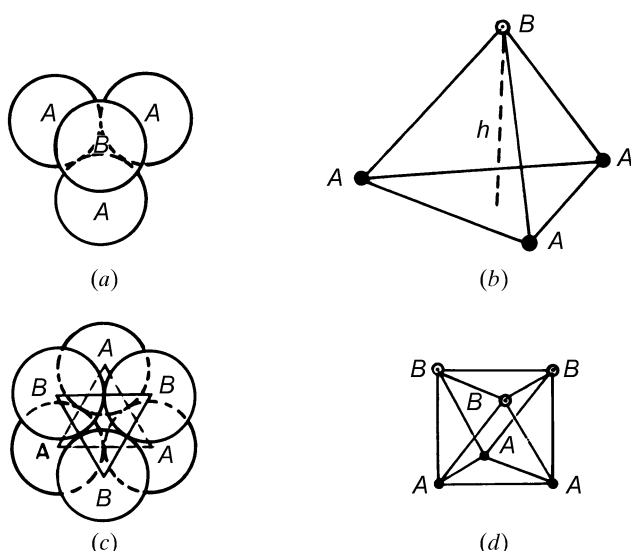


Fig. 9.2.1.3. Voids in a close packing: (a) tetrahedral void; (b) tetrahedron formed by the centres of spheres; (c) octahedral void; (d) octahedron formed by the centres of spheres.

9.2.1.2.1. Voids in close packing

Three-dimensional close packings of spheres have two kinds of voids (Azaroff, 1960):

(i) If the triangular interstices in a close-packed layer have spheres directly over them, the resulting voids are called tetrahedral voids because the four spheres surrounding the void are arranged at the corners of a regular tetrahedron (Figs. 9.2.1.3a,b). If R denotes the radius of the four spheres surrounding a tetrahedral void, the radius of the sphere that would just fit into this void is given by $0.225R$ (Verma & Krishna, 1966). The centre of the tetrahedral void is located at a distance $3h/4$ from the centre of the sphere on top of it.

(ii) If the triangular interstices pointing up in one close-packed layer are covered by triangular interstices pointing down in the adjacent layer, the resulting voids are called octahedral voids (Figs. 9.2.1.3c,d) since the six spheres surrounding each such void lie at the corners of a regular octahedron. The radius of the sphere that would just fit into an octahedral void is given by $0.414R$ (Verma & Krishna, 1966). The centre of this void is located half way between the two layers of spheres.

While there are twice as many tetrahedral voids as the spheres in close packing, the number of octahedral voids is equal to the number of spheres (Krishna & Pandey, 1981).

9.2.1.2.2. Structures of SiC and ZnS

SiC has a binary tetrahedral structure in which Si and C layers are stacked alternately, each carbon layer occupying half the tetrahedral voids between successive close-packed silicon layers. One can regard the structure as consisting of two identical interpenetrating close packings, one of Si and the other of C, with the latter displaced relative to the former along the stacking axis through one fourth of the layer spacing. Since the positions of C atoms are fixed relative to the positions of layers of Si atoms, it is customary to use the letters A , B , and C as representing Si-C double layers in the close packing. To be more exact, the three kinds of layers need to be written as $A\alpha$, $B\beta$, and $C\gamma$ where Roman and Greek letters denote the positions of Si and C atoms, respectively. Fig. 9.2.1.4 depicts the structure of SiC-6H, which is the most common modification.

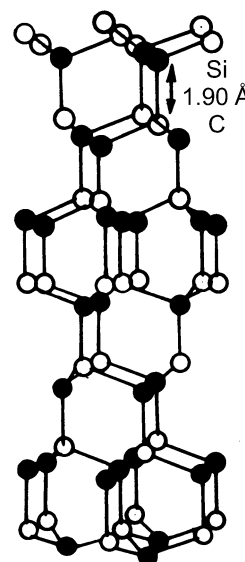


Fig. 9.2.1.4. Tetrahedral arrangement of Si and C atoms in the SiC-6H structure.

9. BASIC STRUCTURAL FEATURES

Table 9.2.1.2. List of SiC polytypes with known structures in order of increasing periodicity (after Pandey & Krishna, 1982a)

Polytype	Structure (Zhdanov sequence)	Polytype	Structure (Zhdanov sequence)
2H	11	57H	(23) ₉ 3333
3C	∞	57R	(33) ₂ 34
4H	22	69R ₁	(33) ₃ 32
6H	33	69R ₂	33322334
8H	44	75R ₂	(32) ₃ (23) ₂
10H	3322	81H	(33) ₅ 35(33) ₆ 34
14H	(22) ₂ 33	84R	(33) ₃ (32) ₂
15R	23	87R	(33) ₄ 32
16H ₁	(33) ₂ 22	90R	(23) ₄ 3322
18H	(22) ₃ 33	93R	(33) ₄ 34
19H	(23) ₃ 22	96R ₁	(33) ₃ 3434
20H	(22) ₃ 44	99R	(33) ₄ 3222
21H	333534	105R	(33) ₅ 32
21H ₂	(33) ₂ 63	111R	(33) ₅ 34
21R	34	120R	(22) ₅ 23222333
24R	35	123R	(33) ₆ 32
27H	(33) ₂ (23) ₃	126R	(33) ₂ 2353433223
27R	2223	129R	(33) ₆ 34
33R	3332	125R	32(33) ₂ 23(33) ₃ 23
33H	(33) ₂ 353334	141R	(33) ₇ 32
34H	(33) ₄ 2332	147R	(3332) ₄ 32
36H ₁	(33) ₂ 32(33) ₂ 34	150R ₁	(23) ₃ 32(23) ₃ 322332
36H ₂	(33) ₄ 3234	150R ₂	(23) ₂ (3223) ₄
39H	(33) ₂ 32(33) ₃ (32) ₂	159R	(33) ₈ 32
39R	3334	168R	(23) ₁₀ 33
40H	(33) ₅ 2332	174R	(33) ₆ 6(33) ₃ 4
45R	(23) ₂ 32	189R	(34) ₈ 43
51R ₁	(33) ₂ 32	267R	(23) ₁₇ 22
51R ₂	(22) ₃ 23	273R	(23) ₁₇ 33
54H	(33) ₆ 323334	393R	(33) ₂₁ 32

A large number of crystallographically different modifications of SiC, called polytypes, has been discovered in commercial crystals grown above 2273 K (Verma & Krishna, 1966; Pandey & Krishna, 1982a). Table 9.2.1.2 lists those polytypes whose structures have been worked out. All these polytypes have $a = b = 3.078 \text{ \AA}$ and $c = n \times 2.518 \text{ \AA}$, where n is the number of Si-C double layers in the hexagonal cell. The 3C and 2H modifications, which normally result below 2273 K, are known to undergo solid-state structural transformation to 6H (Jagodzinski, 1972; Krishna & Marshall, 1971a,b) through a non-random insertion of stacking faults (Pandey, Lele & Krishna, 1980a,b,c; Kabra, Pandey & Lele, 1986). The lattice parameters and the average thickness of the Si-C double layers vary slightly with the structure, as is evident from the h/a ratios of 0.8205 (Adamsky & Merz, 1959), 0.8179, and 0.8165 (Taylor & Jones, 1960) for the 2H, 6H, and 3C structures, respectively. Even in the same structure, crystal-structure refinement has revealed variation in the thickness of Si-C double layers depending on their environment (de Mesquita, 1967).

The structure of ZnS is analogous to that of SiC. Like the latter, ZnS crystals grown from the vapour phase also display a large variety of polytype structures (Steinberger, 1983). ZnS crystals that occur as minerals usually correspond to the wurtzite ($/AB/...$) and the sphalerite ($/ABC/...$) modifications. The structural transformation between the 2H and 3C structures of ZnS is known to be martensitic in nature (Sebastian, Pandey & Krishna, 1982; Pandey & Lele, 1986b). The h/a ratio for ZnS-2H is 0.818, which is somewhat different from the ideal

value (Verma & Krishna, 1966). The structure of the stackings in polytypic AgI is analogous to those in SiC and ZnS (Prager, 1983).

9.2.1.2.3. Structure of CdI₂

The structure of cadmium iodide consists of a close packing of the I ions with the Cd ions distributed amongst half the octahedral voids. Thus, the Cd and I layers are not stacked alternately; there is one Cd layer after every two I layers as shown in Fig. 9.2.1.5. The structure actually consists of molecular sheets (called minimal sandwiches) with a layer of Cd ions sandwiched between two close-packed layers of I ions. The bonding within the minimal sandwich is ionic in character and is much stronger than the bonding between successive sandwiches, which is of van der Waals type. The importance of polarization energy for the stability of such structures has recently been emphasized by Bertaut (1978). It is because of the weak van der Waals bonding between the successive minimal sandwiches that the material possesses the easy cleavage characteristic of a layer structure. In describing the layer stackings in the CdI₂ structure, it is customary to use Roman letters to denote the I positions and Greek letters for the Cd positions. The two most common modifications of CdI₂ are 4H and 2H with layer stackings $A\gamma B C\alpha B \dots$ and $A\gamma B A\gamma B$, respectively. In addition, this material also displays a number of polytype modifications of large repeat periods (Trigunayat & Verma, 1976; Pandey & Krishna, 1982a). From the structure of CdI₂, it follows that the identity period of all such modifications must consist of an even number of I layers. The h/a ratio in all these modifications of CdI₂ is 0.805, which is very different from the ideal value (Verma & Krishna, 1966). The structure of PbI₂, which also displays a large number of polytypes, is analogous to CdI₂ with one important difference. Here, the distances between two I layers with and without an intervening Pb layer are quite different (Trigunayat & Verma, 1976).

9.2.1.2.4. Structure of GaSe

The crystal structure of GaSe consists of four-layered slabs, each of which contains two close-packed layers of Ga (denoted by symbols A, B, C) and Se (denoted by symbols α, β, γ) each in the sequence Se-Ga-Ga-Se (Terhell, 1983). The Se atoms sit on the corners of a trigonal prism while each Ga atom is tetrahedrally coordinated by three Se and one Ga atoms. If the Se layers are of A type, then the stacking sequence of the four

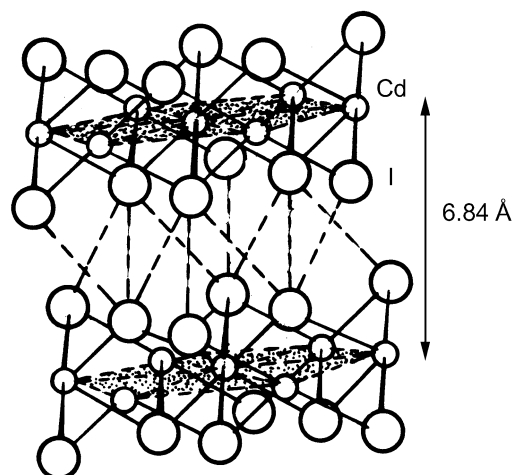


Fig. 9.2.1.5. The layer structure of CdI₂: small circles represent Cd ions and larger ones I ions (after Wells, 1945).

9.2. LAYER STACKING

layers in the slab can be written as $A\beta\beta A$ or $A\gamma\gamma A$. There are thus six possible sequences for the unit slab. These unit slabs can be stacked in the manner described for equal spheres. Thus, for example, the $2H$ structure can have three different layer stackings: $/A\beta\beta A B\gamma\gamma B/\dots$, $/A\beta\beta A B\alpha\alpha B/\dots$ and $/A\beta\beta A C\beta\beta C/$. Periodicities containing up to 21 unit slabs have been reported for GaSe (see Terhell, 1983). The bonding between the layers of a slab is predominantly covalent while that between two adjacent slabs is of the van der Waals type, which imparts cleavage characteristics to this material.

9.2.1.3. Symmetry of close-packed layer stackings of equal spheres

It can be seen from Fig. 9.2.1.2(a) that a stacking of two or more layers in the close-packed manner still possesses all three symmetry planes but the twofold axes disappear while the sixfold axes coincide with the threefold axes (Verma & Krishna, 1966). The lowest symmetry of a completely arbitrary periodic stacking sequence of close-packed layers is shown in Fig. 9.2.1.2(b). Structures resulting from such stackings therefore belong to the trigonal system. Even though a pure sixfold axis of rotation is not possible, close-packed structures belonging to the hexagonal system can result by virtue of at least one of the three symmetry axes parallel to $[00.1]$ being a 6_3 axis (Verma & Krishna, 1966). This is possible if the layers in the unit cell are stacked in special ways. For example, a $6H$ stacking sequence $/ABCACB/\dots$ has a 6_3 axis through $0, 0$. It follows that, for an nH structure belonging to the hexagonal system, n must be even. A packing nH/nR with n odd will therefore necessarily belong to the trigonal system and can have either a hexagonal or a rhombohedral lattice (Verma & Krishna, 1966).

Other symmetries that can arise by restricting the arbitrariness of the stacking sequence in the identity period are: (i) a centre of symmetry at the centre of either the spheres or the octahedral voids; and (ii) a mirror plane perpendicular to $[00.1]$. Since there must be two centres of symmetry in the unit cell, the centrosymmetric arrangements may possess both centres either at sphere centres/octahedral void centres or one centre each at the centres of spheres and octahedral voids (Patterson & Kasper, 1959).

9.2.1.4. Possible lattice types

Close packings of equal spheres can belong to the trigonal, hexagonal, or cubic crystal systems. Structures belonging to the hexagonal system necessarily have a hexagonal lattice, *i.e.* a lattice in which we can choose a primitive unit cell with $a = b \neq c$, $\alpha = \beta = 90^\circ$, and $\gamma = 120^\circ$. In the primitive unit cell of the hexagonal close-packed structure $/AB/\dots$ shown in Fig. 9.2.1.6, there are two spheres associated with each lattice point, one at $0, 0, 0$ and the other at $\frac{1}{3}, \frac{2}{3}, \frac{1}{2}$. Structures belonging to the trigonal system can have either a hexagonal or a rhombohedral lattice. By a rhombohedral lattice is meant a lattice in which we can choose a primitive unit cell with $a = b = c$, $\alpha = \beta = \gamma \neq 90^\circ$. Both types of lattice can be referred to either hexagonal or rhombohedral axes, the unit cell being non-primitive when a hexagonal lattice is referred to rhombohedral axes and *vice versa* (Buerger, 1953). In close-packed structures, it is generally convenient to refer both hexagonal and rhombohedral lattices to hexagonal axes. Fig. 9.2.1.7 shows a rhombohedral lattice in which the primitive cell is defined by the rhombohedral axes a_1, a_2, a_3 ; but a non-primitive hexagonal unit cell can be chosen by adopting the axes A_1, A_2, C . The latter has lattice points at $0, 0, 0$; $\frac{2}{3}, \frac{1}{3}, \frac{1}{3}$; and $\frac{1}{3}, \frac{2}{3}, \frac{2}{3}$. If this rhombohedral lattice is rotated through 60° around

$[00.1]$, the hexagonal unit cell will then be centred at $\frac{1}{3}, \frac{2}{3}, \frac{1}{3}$ and $\frac{2}{3}, \frac{1}{3}, \frac{2}{3}$. These two settings are crystallographically equivalent for close packing of equal spheres. They represent twin arrangements when both occur in the same crystal. The hexagonal unit cell of an nR structure is made up of three elementary stacking sequences of $n/3$ layers that are related to each other either by an anticyclic shift of layers $A \rightarrow C \rightarrow B \rightarrow A$ (obverse setting) or by a cyclic shift of layers $A \rightarrow B \rightarrow C \rightarrow A$ (reverse setting) in the direction of z increasing (Verma & Krishna, 1966). Evidently, n must be a multiple of 3 for nR structures.

In the special case of the close packing $/ABC/\dots$ [with the ideal axial ratio of $\sqrt{(2/3)}$], the primitive rhombohedral unit cell has $\alpha = \beta = \gamma = 60^\circ$, which enhances the symmetry and enables the choice of a face-centred cubic unit cell. The relationship between the face-centred cubic and the rhombohedral unit cell is shown in Fig. 9.2.1.8. The threefold axis of the rhombohedral unit cell coincides with one of the $\langle 111 \rangle$ directions of the cubic unit cell. The close-packed layers are thus parallel to the $\{111\}$ planes in the cubic close packing.

9.2.1.5. Possible space groups

It was shown by Belov (1947) that consistent combinations of the possible symmetry elements in close packing of equal spheres can give rise to eight possible space groups: $P3m1$, $P\bar{3}m1$,

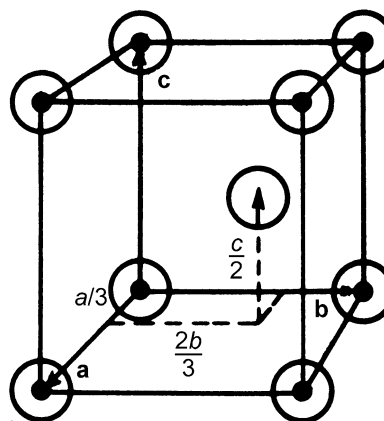


Fig. 9.2.1.6. The primitive unit cell of the $2H$ close packing.

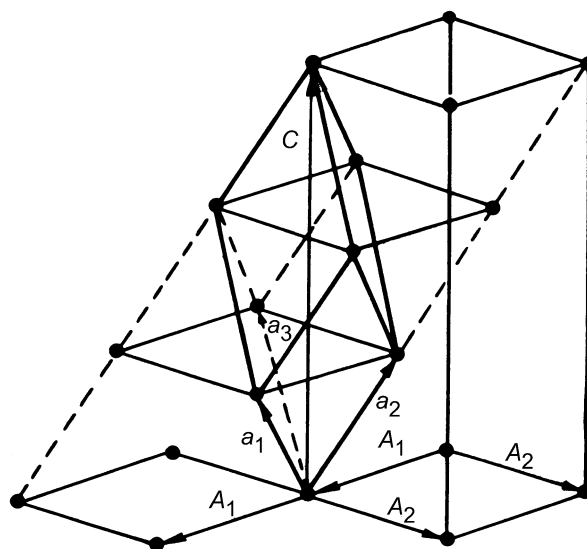


Fig. 9.2.1.7. A rhombohedral lattice (a_1, a_2, a_3) referred to hexagonal axes (A_1, A_2, C) (after Buerger, 1953).

9. BASIC STRUCTURAL FEATURES

$P\bar{6}m2$, $P6_3mc$, $P6_3/mmc$, $R3m$, $R\bar{3}m$, and $Fm\bar{3}m$. The last space group corresponds to the special case of cubic close packing $/ABC/ \dots$. The tetrahedral arrangement of Si and C in SiC does not permit either a centre of symmetry ($\bar{1}$) or a plane of symmetry (m) perpendicular to $[00.1]$. SiC structures can therefore have only four possible space groups $P3m1$, $R3m1$, $P6_3mc$, and $F\bar{4}3m$. CdI_2 structures can have a centre of symmetry on octahedral voids, but cannot have a symmetry plane perpendicular to $[00.1]$. CdI_2 can therefore have five possible space groups: $P3m1$, $P\bar{3}m$, $R3m$, $R\bar{3}m$, and $P6_3mc$. Cubic symmetry is not possible in CdI_2 on account of the presence of Cd atoms, the sequence $/A\gamma BC\beta AB\alpha C/$ representing a $6R$ structure.

9.2.1.6. Crystallographic uses of Zhdanov symbols

From the Zhdanov symbols of a close-packed structure, it is possible to derive information about the symmetry and lattice type (Verma & Krishna, 1966). Let n_+ and n_- be the number of positive and negative numerals in the Zhdanov sequence of a given structure. The lattice is rhombohedral if $n_+ - n_- = \pm 1 \pmod 3$, otherwise it is hexagonal. The $+$ sign corresponds to the reverse setting and $-$ to the obverse setting of the rhombohedral lattice. Since this criterion is sufficient for the identification of a rhombohedral structure, the practice of writing three units of identical Zhdanov symbols has been abandoned in recent years (Pandey & Krishna, 1982a). Thus the $15R$ polytype of SiC is written as (23) rather than (23)₃.

As described in detail by Verma & Krishna (1966), if the Zhdanov symbol consists of an odd set of numbers repeated twice, e.g. (22), (33), (221221) etc., the structure can be shown to possess a 6_3 axis. For the centre of symmetry at the centre of a sphere or an octahedral void, the Zhdanov symbol will consist of a symmetrical arrangement of numbers of like signs surrounding a single even or odd Zhdanov number, respectively. Thus, the structures (2)32(4)23 and (3)32(5)23 have centres of symmetry of the two types in the numbers within parentheses. For structures with a symmetry plane perpendicular to $[00.1]$, the Zhdanov symbols consist of a symmetrical arrangement of a set of numbers of opposite signs about the space between two succession numbers. Thus, a stacking $|522|225|$ has mirror planes at positions indicated by the vertical lines.

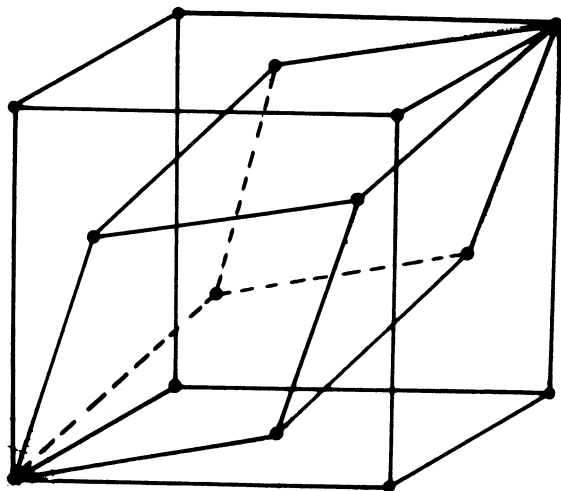


Fig. 9.2.1.8. The relationship between the f.c.c. and the primitive rhombohedral unit cell of the c.c.p. structure.

The use of abridged symbols to describe crystal structures has sometimes led to confusion in deciding the crystallographic equivalence of two polytype structures. For example, the structures (13) and (31) are identical for SiC but not for CdI_2 (Jain & Trigunayat, 1977a,b).

9.2.1.7. Structure determination of close-packed layer stackings

9.2.1.7.1. General considerations

The different layer stackings (polytypes) of the same material have identical a and b parameters of the direct lattice. The a^*b^* reciprocal-lattice net is therefore also the same and is shown in Fig. 9.2.1.9. The reciprocal lattices of these polytypes differ only along the c^* axis, which is perpendicular to the layers. It is evident from Fig. 9.2.1.9 that for each reciprocal-lattice row parallel to c^* there are five others with the same value of the radial coordinate ξ . For example, the rows $10.l$, $01.l$, $\bar{1}1.l$, $\bar{1}0.l$, $0\bar{1}.l$, and $1\bar{1}.l$ all have $\xi = |a^*|$. Owing to symmetry considerations, it is sufficient to record any one of them on X-ray diffraction photographs. The reciprocal-lattice rows hkl can be classified into two categories according as $h - k = 0 \pmod 3$ or $\pm 1 \pmod 3$. Since the atoms in an nH or nR structure lie on three symmetry axes $A : [00.1]_{00}$, $B : [00.1]_{\frac{1}{3}, -\frac{1}{3}}$, and $C : [00.1]_{-\frac{1}{3}, \frac{1}{3}}$, the structure factor F_{hkl} can be split into three parts:

$$F_{hkl} = P + Q \exp[2\pi i(h - k)/3] + R \exp[-2\pi i(h - k)/3],$$

where $P = \sum_{z_A} \exp(2\pi i l z_A/n)$, $Q = \sum_{z_B} \exp(2\pi i l z_B/n)$, $R = \sum_{z_C} \exp(2\pi i l z_C/n)$, and z_A/n , z_B/n , z_C/n are the z coordinates of atoms at A , B , and C sites, respectively. For $h - k = 0 \pmod 3$,

$$F_{hkl} = P + Q + R = \sum_{z=0}^{n-1} \exp(2\pi i l z/n),$$

which is zero except when $l = 0, n, 2n, \dots$. Hence, the reflections $00.l$, $11.l$, $30.l$, etc., for which $h - k = 0 \pmod 3$, will be extinguished except when $l = 0, n, 2n, \dots$. Thus, only those hkl reciprocal-lattice rows for which $h - k \neq 0 \pmod 3$ carry information about the stacking sequence and contain in general reflections with $l = 0, 1, 2, \dots, n - 1$, etc. It is sufficient to record any one such row, usually the $10.l$ row with $\xi = |a^*|$, on an oscillation, Weissenberg, or precession photograph to obtain information about the lattice type, identity period, space group, and hence the complete structure (Verma & Krishna, 1966).

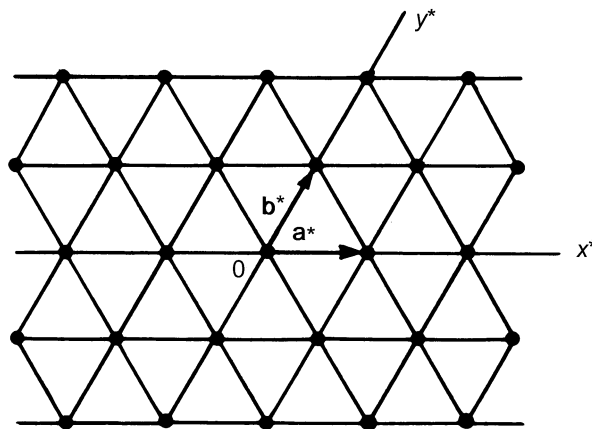


Fig. 9.2.1.9. The a^*b^* reciprocal-lattice net for close-packed layer stackings.

9.2. LAYER STACKING

9.2.1.7.2. Determination of the lattice type

When the structure has a hexagonal lattice, the positions of spots are symmetrical about the zero layer line on the c -axis oscillation photograph. However, the intensities of the reflections on the two sides of the zero layer line are the same only if the structure possesses a 6_3 axis, and not for the trigonal system. An apparent mirror symmetry perpendicular to the c axis results from the combination of the 6_3 axis with the centre of symmetry introduced by X-ray diffraction. For a structure with a rhombohedral lattice, the positions of X-ray diffraction spots are not symmetrical about the zero layer line because the hexagonal unit cell is non-primitive causing the reflections hkl to be absent when $-h + k + l \neq 3n$ ($\pm n = 0, 1, 2, \dots$). For the $10.l$ row, this means that the permitted reflections will have $l = 3n + 1$, which implies above the zero layer line $10.1, 10.4, 10.7, \text{etc.}$ reflections and below the zero layer line $10.\bar{2}, 10.\bar{5}, 10.\bar{8}, \text{etc.}$ The zero layer line will therefore divide the distance between the nearest spots on either side (namely 10.1 and $10.\bar{2}$) approximately in the ratio 1:2. This enables a quick identification of a rhombohedral lattice. It is also possible to identify rhombohedral lattices by the appearance of an apparent 'doubling' of spots along the Bernal row lines on a rotation photograph. This is because of the threefold symmetry which makes reciprocal-lattice rows such as $10.l, \bar{1}1.l, \text{and } 0\bar{1}.l$ identical with each other but different from the other identical set, $01.l, \bar{1}0.l, \text{and } 1\bar{1}.l$. The extinction condition for the second set requires $l = 3n - 1$, *i.e.* $l = 2, 5, 8, \text{and } \bar{1}, \bar{4}, \bar{7}, \text{etc.}$, which is different from that for the first set. Consequently, on the rotation photograph, reciprocal-lattice rows with $\xi = |a^*|$ will have spots for $l = 3n \pm 1$ causing the apparent 'doubling'.

In crystals of layer structures, such as CdI_2 , where a -axis oscillation photographs are normally taken, the identification of the rhombohedral lattice is performed by checking for the non-coincidence of the diffraction spots with those for the $2H$ or $4H$ structures. In an alternative method, one compares the positions of spots in two rows of the type $10.l$ and $20.l$. This can conveniently be done by taking a Weissenberg photograph (Chadha, 1977).

9.2.1.7.3. Determination of the identity period

The number of layers, n , in the hexagonal unit cell can be found by determining the c parameter from the c -axis rotation or oscillation photographs and dividing this by the layer spacing h for that compound which can be found from reflections with $h - k = 0 \pmod{3}$. The density of reciprocal-lattice points along rows parallel to c^* depends on the periodicity along the c axis. The larger the identity period along c , the more closely spaced are the diffraction spots along c^* . In situations where there are not many structural extinctions, n can be determined by counting the number of spacings after which the sequence of relative intensities begins to repeat along the $10.l$ row of spots on an oscillation or Weissenberg photograph (Krishna & Verma, 1963). If the structure contains a random stacking disorder of close-packed layers (stacking faults), this will effectively make the c parameter infinite ($c^* \rightarrow 0$) and lead to the production of characteristic continuous diffuse streaks along reciprocal-lattice rows parallel to c^* for reflections with $h - k \neq 0 \pmod{3}$ (Wilson, 1942). It is therefore difficult to distinguish by X-ray diffraction between structures of very large unresolvable periodicities and those with random stacking faults. Lattice resolution in the electron microscope has been used in recent years to identify such structures (Dubey, Singh & Van Tendeloo, 1977). A better resolution of diffraction spots along the $10.l$ reciprocal-lattice row can be obtained by using the Laue method. Standard charts

for rapid identification of SiC polytypes from Laue films are available in the literature (Mitchell, 1953). Identity periods as large as 594 layers have been resolved by this method (Honjo, Miyake & Tomita, 1950). Synchrotron radiation has been used for taking Laue photographs of ZnS polytypes (Steinberger, Bordas & Kalman, 1977).

9.2.1.7.4. Determination of the stacking sequence of layers

For an nH or $3nR$ polytype, the n close-packed layers in the unit cell can be stacked in 2^{n-1} possible ways, all of which cannot be considered for ultimate intensity calculations. A variety of considerations has therefore been used for restricting the number of trial structures. To begin with, symmetry and space-group considerations discussed in Subsection 9.2.1.4 and 9.2.1.5 can considerably reduce the number of trial structures.

When the short-period structures act as 'basic structures' for the generation of long-period polytypes, the number of trial structures is considerably reduced since the crystallographic unit cells of the latter will contain several units of the small-period structures with faults between or at the end of such units. The basic structure of an unknown polytype can be guessed by noting the intensities of $10.l$ reflections that are maximum near the positions corresponding to the basic structure. If the unknown polytype belongs to a well known structure series, such as $(33)_n32$ and $(33)_n34$ based on SiC- $6H$, empirical rules framed by Mitchell (1953) and Krishna & Verma (1962) can allow the direct identification of the layer-stacking sequence without elaborate intensity calculations.

It is possible to restrict the number of probable structures for an unknown polytype on the basis of the faulted matrix model of polytypism for the origin of polytype structures (for details see Pandey & Krishna, 1983). The most probable series of structures as predicted on the basis of this model for SiC contains the numbers 2, 3, 4, 5 and 6 in their Zhdanov sequence (Pandey & Krishna, 1975, 1976a). For CdI_2 and PbI_2 polytypes, the possible Zhdanov numbers are 1, 2 and 3 (Pandey & Krishna, 1983; Pandey, 1985). On the basis of the faulted matrix model, it is not only possible to restrict the numbers occurring in the Zhdanov sequence but also to restrict drastically the number of trial structures for a new polytype.

Structure determination of ZnS polytypes is more difficult since they are not based on any simple polytype and any number can appear in the Zhdanov sequence. It has been observed that the birefringence of polytype structures in ZnS varies linearly with the percentage hexagonality (Brafman & Steinberger, 1966), which in turn is related to the number of reversals in the stacking sequence, *i.e.* the number of numbers in the Zhdanov sequence. This drastically reduces the number of trial structures for ZnS (Brafman, Alexander & Steinberger, 1967).

Singh and his co-workers have successfully used lattice imaging in conjunction with X-ray diffraction for determining the structures of long-period polytypes of SiC that are not based on a simple basic structure. After recording X-ray diffraction patterns, single crystals of these polytypes were crushed to yield electron-beam-transparent flakes. The one- and two-dimensional lattice images were used to propose the possible structures for the polytypes. Usually this approach leads to a very few possibilities and the correct structure is easily determined by comparing the observed and calculated X-ray intensities for the proposed structures (Dubey & Singh, 1978; Rai, Singh, Dubey & Singh, 1986).

Direct methods for the structure determination of polytypes from X-ray data have also been suggested by several workers (Tokonami & Hosoya, 1965; Dornberger-Schiff & Farkas-

9. BASIC STRUCTURAL FEATURES

Jahnke, 1970; Farkas-Jahnke & Dornberger-Schiff, 1969) and have been reviewed by Farkas-Jahnke (1983). These have been used to derive the structures of ZnS, SiC, and TiS_{1.7} polytypes. These methods are extremely sensitive to experimental errors in the intensities.

9.2.1.8. Stacking faults in close-packed structures

The two alternative positions for the stacking of successive close-packed layers give rise to the possibility of occurrence of faults where the stacking rule is broken without violating the law of close packing. Such faults are frequently observed in crystals of polytypic materials as well as close-packed martensites of cobalt, noble-metal-based and certain iron-based alloys (Andrade, Chandrasekaran & Delaey 1984; Kabra, Pandey & Lele, 1988a; Nishiyama, 1978; Pandey, 1988).

The classical method of classifying stacking faults in 2H and 3C structures as growth and deformation types, depending on whether the fault has resulted as an accident during growth or by shear through the vector *s*, leads to considerable ambiguities since the same fault configuration can result from more than one physical process. For a detailed account of the limitations of the notations based on the process of formation, the reader is referred to the articles by Pandey (1984a) and Pandey & Krishna (1982b).

Frank (1951) has classified stacking faults as intrinsic or extrinsic purely on geometrical considerations. In intrinsic faults, the perfect stacking sequence on each side of the fault extends right up to the contact plane of the two crystal halves while in extrinsic faults the contact plane does not belong to the stacking sequence on either side of it. In intrinsic faults, the contact plane may be an atomic or non-atomic plane whereas in extrinsic faults the contact plane is always an atomic plane. Instead of contact plane, one can use the concept of fault plane defined with respect to the initial stacking sequence. This system of classification is preferable to that based on the process of formation. However, the terms intrinsic and extrinsic have been used in the literature in a very restricted sense by associating these with the precipitation of vacancies and interstitials, respectively (see, for example, Weertman & Weertman, 1984). While the precipitation of vacancies may lead to intrinsic fault configuration, this is by no means the only process by which intrinsic faults can result. For example, there are geometrically 18 possible intrinsic fault configurations in the 6H (33) structure (Pandey & Krishna, 1975) but only two of these can result from the precipitation of vacancies. Similarly, layer-displacement faults involved in SiC transformations are extrinsic type but do not result from the precipitation of interstitials (see Pandey, Lele & Krishna, 1980a,b,c; Kabra, Pandey & Lele, 1986). It is therefore desirable not to associate the geometrical notation of Frank with any particular process of formation.

The intrinsic-extrinsic scheme of classification of faults when used in conjunction with the concept of assigning subscripts to different close-packed layers (Prasad & Lele, 1971; Pandey & Krishna, 1976b) can provide a very compact and unique way of representing intrinsic fault configurations even in long-period structures (Pandey, 1984b). We shall briefly explain this notation in relation to one hexagonal (6H) and one rhombohedral (9R) structure.

In the 6H (ABCACB, ... or hkhk) structure, six kinds of layers that can be assigned subscripts 0, 1, 2, 3, 4, and 5 need to be distinguished (Pandey, 1984b). Choosing the 0-type layer in 'h' configuration such that the layer next to it is related through

Table 9.2.1.3. *Intrinsic fault configurations in the 6H (A₀B₁C₂A₃C₄B₅, ...) structure*

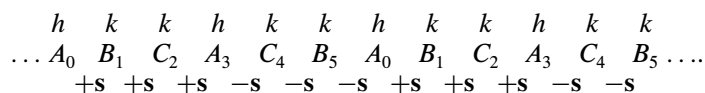
Fault configuration ABC sequence	Subscript notation
... A B C A C B A ₀ C ₀ A B C B A C ...	<i>I</i> _{0,0}
... A B C A C B A ₀ C ₁ A B A C B C ...	<i>I</i> _{0,1}
... A B C A C B A ₀ C ₂ A C B A B C ...	<i>I</i> _{0,2}
... A B C A C B A ₀ C ₃ B A C A B C ...	<i>I</i> _{0,3}
... A B C A C B A ₀ C ₄ B A B C A C ...	<i>I</i> _{0,4}
... A B C A C B A ₀ C ₅ B C A B A C ...	<i>I</i> _{0,5}
... A B C A C B A B ₁ A ₀ B C A C B A ...	<i>I</i> _{1,0}
... A B C A C B A B ₁ A ₁ B C B A C A ...	<i>I</i> _{1,1}
... A B C A C B A B ₁ A ₂ B A C B C A ...	<i>I</i> _{1,2}
... A B C A C B A B ₁ A ₃ C B A B C A ...	<i>I</i> _{1,3}
... A B C A C B A B ₁ A ₄ C B C A B A ...	<i>I</i> _{1,4}
... A B C A C B A B ₁ A ₅ C A B C B A ...	<i>I</i> _{1,5}
... A B C A C B A B C ₂ B ₀ C A B A C B ...	<i>I</i> _{2,0}
... A B C A C B A B C ₂ B ₁ C A C B A B ...	<i>I</i> _{2,1}
... A B C A C B A B C ₂ B ₂ C B A C A B ...	<i>I</i> _{2,2}
... A B C A C B A B C ₂ B ₃ A C B C A B ...	<i>I</i> _{2,3}
... A B C A C B A B C ₂ B ₄ A C A B C B ...	<i>I</i> _{2,4}
... A B C A C B A B C ₂ B ₅ A B C A C B ...	<i>I</i> _{2,5}

Notes:

(1) Dotted vertical lines represent the location of the fault plane with respect to the initial stacking sequence on the left-hand side.

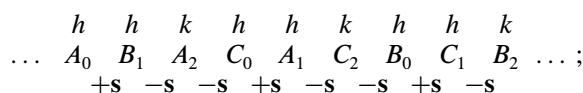
(2) *I*_{0,1} and *I*_{2,3}, *I*_{0,2} and *I*_{1,3}, *I*_{1,1} and *I*_{2,2}, and *I*_{1,4} and *I*_{2,5} are crystallographically equivalent.

the shift vector +*s* (which causes cyclic *A* → *B* → *C* → *A* shift), the perfect 6H structure can be written as



There are six crystallographically equivalent ways of writing this structure with the first layer in position *A*: (i) *A*₀*B*₁*C*₂*A*₃*C*₄*B*₅; (ii) *A*₁*B*₂*C*₃*B*₄*A*₅*C*₀; (iii) *A*₂*B*₃*A*₄*C*₅*B*₀*C*₁; (iv) *A*₃*C*₄*B*₅*A*₀*B*₁*C*₂; (v) *A*₄*C*₅*B*₀*C*₁*A*₂*B*₃; and (vi) *A*₅*C*₀*A*₁*B*₂*C*₃*B*₄. Similarly, there are six ways of writing the 6H structure with the starting layer in position *B* or *C*. Since an intrinsic fault marks the beginning of a fresh 6H sequence, there can be 36 possible intrinsic fault configurations in the 6H (ABCACB, ...) structure. All these intrinsic fault configurations can be described by symbols like *I*_{*r,s*}, where *r* and *s* stand for the subscript of the layer on the left- and right-hand sides of the fault plane while *I* represents intrinsic. Knowing the two symbols (*r* and *s*), one can write down the complete ABC stacking sequence. It may be noted that, of the 36 possible intrinsic fault configurations, only 14 are crystallographically indistinguishable (for details, see Pandey, 1984b). This notation can be used for any hexagonal polytype and requires only the identification of various layer types in the structure. For rhombohedral polytypes, one must consider the layer types in both the obverse and the reverse settings. For example, six layer types need to be distinguished in the 9R (hkh) structure:

Obverse:



9.2. LAYER STACKING

Table 9.2.1.4. *Intrinsic fault configurations in the 9R (A₀B₁A₂C₀A₁C₂B₀C₁B₂, ...) structure*

Fault configuration ABC sequence	Subscript notation
... A B A C A C B C B A ₀ C ₀ A C B C B A B A ...	I _{0,0}
... A B A C A C B C B A ₀ C ₁ B A B A C A C B ...	I _{0,1}
... A B A C A C B C B A ₀ C ₂ B C B A B A C A ...	I _{0,2}
... A B A C A C B C B A ₀ C ₀ B C A C A B A B ...	I _{0,0̄}
... A B A C A C B C B A ₀ C ₁ A B A B C B C A ...	I _{0,1̄}
... A B A C A C B C B A ₀ C ₂ A C A B A B C B ...	I _{0,2̄}
... A B A C A C B C B A B ₁ C ₀ A C B C B A B A ...	I _{1,0}
... A B A C A C B C B A B ₁ C ₁ B A B A C A C B ...	I _{1,1}
... A B A C A C B C B A B ₁ C ₂ B C B A B A C A ...	I _{1,2}
... A B A C A C B C B A B ₁ C ₀ B C A C A B A B ...	I _{1,0̄}
... A B A C A C B C B A B ₁ C ₁ A B A B C B C A ...	I _{1,1̄}
... A B A C A C B C B A B ₁ C ₂ A C A B A B C B ...	I _{1,2̄}
... A B A C A C B C B A B A ₂ B ₀ C B A B A C A C ...	I _{2,0}
... A B A C A C B C B A B A ₂ B ₁ A C A C B C B A ...	I _{2,1}
... A B A C A C B C B A B A ₂ B ₂ A B A C A C B C ...	I _{2,2}
... A B A C A C B C B A B A ₂ B ₀ A B C B C A C A ...	I _{2,0̄}
... A B A C A C B C B A B A ₂ B ₁ C A C A B A B C ...	I _{2,1̄}
... A B A C A C B C B A B A ₂ B ₂ C B C A C A B A ...	I _{2,2̄}

Note: I_{0,0̄} and I_{1,1̄}, I_{0,1̄} and I_{1,2̄}, I_{0,2̄} and I_{2,1̄}, and I_{1,2} and I_{2,0} are crystallographically equivalent.

Reverse:

$$\begin{array}{cccccccc}
 h & h & k & h & h & k & h & h & k \\
 \dots & A_0 & C_1 & A_2 & B_0 & A_1 & B_2 & C_0 & B_1 & C_2 & \dots \\
 -s & +s & +s & -s & +s & +s & -s & +s &
 \end{array}$$

In the obverse setting, we choose the origin layer (0 type) in the *h* configuration such that the next layer is cyclically shifted whereas in the reverse setting the origin layer (0 type) in the *h* configuration is related to the next layer through an anticyclic shift. Tables 9.2.1.3 and 9.2.1.4 list the crystallographically unique intrinsic fault configurations in the 6H and 9R structures.

9.2.1.8.1. *Structure determination of one-dimensionally disordered crystals*

Statistical distribution of stacking faults in close-packed structures introduces disorder along the stacking axis of the close-packed layers. As a result, one observes on a single-crystal diffraction pattern not only normal Bragg scattering near the nodes of the reciprocal lattice of the average structure but also continuous diffuse scattering between the nodes owing to the incomplete destructive interference of scattered rays. Just like the extra polytype reflections, the diffuse streaks are also confined to only those rows for which $h - k \neq 0 \pmod{3}$. A complete description of the real structure of such one-dimensionally disordered polytypes requires knowledge of the average structure as well as a statistical specification of the fluctuations due to stacking faults in the electron-density distribution of the average structure. This cannot be accomplished by the usual consideration of the normal Bragg reflections alone but requires a careful analysis of the diffuse intensity distribution as well (Pandey, Kabra & Lele, 1986).

The first step in the structure determination of one-dimensionally disordered structures is the specification of the geometry of stacking faults and their distribution, both of which require postulation of the physical processes responsible for their formation. An entirely random distribution of faults may result during the layer-by-layer growth of a

crystal (Wilson, 1942) or during plastic deformation (Paterson, 1952). On the other hand, when faults bring about the change in the stacking sequence of layers during solid-state transformations, their distribution is non-random (Pandey, Lele & Krishna, 1980*a,b,c*; Pandey & Lele, 1986*a,b*; Kabra, Pandey & Lele, 1986). Unlike growth faults, which are accidentally introduced in a sequential fashion from one end of the stack of layers to the other during the actual crystal growth, stacking faults involved in solid-state transformations are introduced in a random space and time sequence (Kabra, Pandey & Lele, 1988*b*). Since the pioneering work of Wilson (1942), several different techniques have been advanced for the calculation of intensity distributions along diffuse streaks making use of Markovian chains, random walk, stochastic matrices, and the Paterson function for random and non-random distributions of stacking faults on the assumption that these are introduced in a sequential fashion (Hendricks & Teller, 1942; Jagodzinski 1949*a,b*; Kakinoki & Komura, 1954; Johnson, 1963; Prasad & Lele, 1971; Cowley, 1976; Pandey, Lele & Krishna, 1980*a,b*). The limitations of these methods for situations where non-randomly distributed faults are introduced in the random space and time sequence have led to the use of Monte Carlo techniques for the numerical calculation of pair correlations whose Fourier transforms directly yield the intensity distributions (Kabra & Pandey, 1988).

The correctness of the proposed model for disorder can be verified by comparing the theoretically calculated intensity distributions with those experimentally observed. This step is in principle analogous to the comparison of the observed Bragg intensities with those calculated for a proposed structure in the structure determination of regularly ordered layer stackings. This comparison cannot, however, be performed in a straightforward manner for one-dimensionally disordered crystals due to special problems in the measurement of diffuse intensities using a single-crystal diffractometer, stemming from incident-beam divergence, finite size of the detector slit, and multiple scattering. The problems due to incident-beam divergence in the measurement of the diffuse intensity distributions were first

9. BASIC STRUCTURAL FEATURES

pointed out by Pandey & Krishna (1977) and suitable correction factors have recently been derived by Pandey, Prasad, Lele & Gauthier (1987). A satisfactory solution to the problem of structure determination of one-dimensionally disordered stackings must await proper understanding of all other factors that may influence the true diffraction profiles.

9.2.2. Layer stacking in general polytypic structures (By S. Durovič)

9.2.2.1. *The notion of polytypism*

The common property of the structures described in Section 9.2.1 was the stacking ambiguity of adjacent layer-like structural units. This has been explained by the geometrical properties of close packing of equal spheres, and the different modifications thus obtained have been called *polytypes*.

This phenomenon was first recognized by Baumhauer (1912, 1915) as a result of his investigations of many SiC single crystals by optical goniometry. Among these, he discovered three *types* and his observations were formulated in five statements:

(1) all three types originate simultaneously in the same melt and seemingly also under the same, or nearly the same, conditions;

(2) they can be related in a simple way to the same axial ratio (each within an individual primary series);

(3) any two types (I and II, II and III) have certain faces in common but, except the basal face, there is no face occurring simultaneously in all three types;

(4) the crystals belonging to different, but also to all three, types often form intergrowths with parallel axes;

(5) any of the three types exhibits a typical X-ray diffraction pattern and thus also an individual molecular or atomic structure.

Baumhauer recognized the special role of these *types* within modifications of the same substance and called this phenomenon *polytypism* – a special case of polymorphism. The later determination of the crystal structures of Baumhauer's three types indicated that his results can be interpreted by a family of structures consisting of identical layers with hexagonal symmetry and differing only in their stacking mode.

The stipulation that the individual polytypes grow from the same system and under (nearly) the same conditions influenced for years the investigation of polytypes because it logically led to the question of their growth mechanism.

In the following years, many new polytypic substances have been found. Their crystal structures revealed that polytypism is restricted neither to close packings nor to heterodesmic 'layered structures' (e.g. CdI₂ or GaSe; cf. homodesmic SiC or ZnS; see §§9.2.1.2.2 to 9.2.1.2.4), and that the reasons for a stacking ambiguity lie in the crystal chemistry – in all cases the geometric nearest-neighbour relations between adjacent layers are preserved. The preservation of the bulk chemical composition was not questioned.

Some discomfort has arisen from refinements of the structures of various phyllosilicates. Here especially the micas exhibit a large variety of isomorphous replacements and it turns out that a certain chemical composition stabilizes certain polytypes, excludes others, and that the layers constituting polytypic structures need not be of the same kind. But subsequently the opinion prevailed that the sequence of individual kinds of layers in polytypes of the same family should remain the same and that the relative positions of adjacent layers cannot be completely random (e.g. Zvyagin, 1988). The postulates declared mixed-layer and turbostratic structures as non-polytypic. All this led to certain controversies about the notion of polytypism. While

Thompson (1981) regards polytypes as 'arising through different ways of stacking structurally compatible tabular units ... [provided that this] ... should not alter the chemistry of the crystal as a whole', Angel (1986) demands that 'polytypism arises from different modes of stacking of one or more structurally compatible modules', dropping thus any chemical constraints and allowing also for rod- and block-like modules.

The present official definition (Guinier *et al.*, 1984) reads:

"An element or compound is *polytypic* if it occurs in several different structural modifications, each of which may be regarded as built up by stacking layers of (nearly) identical structure and composition, and if the modifications differ only in their stacking sequence. Polytypism is a special case of polymorphism: the two-dimensional translations within the layers are (essentially) preserved whereas the lattice spacings normal to the layers vary between polytypes and are indicative of the stacking period. No such restrictions apply to polymorphism.

Comment: The above definition is designed to be sufficiently general to make polytypism a useful concept. There is increasing evidence that some polytypic structures are characterized either by small deviations from stoichiometry or by small amounts of impurities. (In the case of certain minerals like clays, micas and ferrites, deviations in composition up to 0.25 atoms per formula unit are permitted within the same polytypic series: two layer structures that differ by more than this amount should not be called polytypic.) Likewise, layers in different polytypic structures may exhibit slight structural differences and may not be isomorphic in the strict crystallographic sense.

The *Ad-Hoc* Committee is aware that the definition of polytypism above is probably too wide since it includes, for example, the turbostratic form of graphite as well as mixed-layer phyllosilicates. However, the sequence and stacking of layers in a polytype are always subject to well-defined limitations. On the other hand, a more general definition of polytypism that includes 'rod' and 'block' polytypes may become necessary in the future."

This definition was elaborated as a compromise between members of the IUCr *Ad-Hoc* Committee on the Nomenclature of Disordered, Modulated and Polytype Structures. It is a slightly modified definition proposed by the IMA/IUCr Joint Committee on Nomenclature (Bailey *et al.*, 1977), which was the target of Angel's (1986) objections.

The official definition has indeed its shortcomings, but not so much in its restrictiveness concerning the chemical composition and structural rigidity of layers, because this can be overcome by a proper degree of abstraction (see below). More critical is the fact that it is not 'geometric' enough. It specifies neither the 'layers' (except for their two-dimensional periodicity), nor the limitations concerning their sequence and stacking mode, and it does not state the conditions under which a polytype belongs to a family.

Very impressive evidence that even polytypes that are in keeping with the first Baumhauer's statement may not have exactly the same composition and the structure of their constituting layers *cannot* be identical has been provided by studies on SiC carried out at the Leningrad Electrotechnical Institute (Sorokin, Tairov, Tsvetkov & Chernov, 1982; Tsvetkov, 1982). They indicate also that each periodic polytype is *sensu stricto* an individual polymorph. Therefore, it appears that the question whether some *real* polytypes belong to the same